6-D BEAM DYNAMICS STUDIES IN EMMA FFAG

F. Méot, DAPNIA & LPSC, Grenoble

Abstract

We report on beam dynamics studies concerning the EMMA electron model of a muon non-scaling FFAG for the Neutrino Factory.

INTRODUCTION

EMMA (Electron Model of a Muon Accelerator) [1] is a design of a 10 to 20 MeV electron model of the linear "fixed field alternating gradient" accelerators (FFAG in the following) proposed for the acceleration to 20 GeV of muons in the neutrino factory (NuFact) [2].

EMMA is supposed to accelerate an electron bunch with large transverse size (several 100π mm.mrad range, norm.) and large longitudinal emittance, based on a strongly nonlinear out of bucket dynamics method (details are given in the following), with non-negligible coupling to transverse motion at large amplitude. From the point of vue of design studies and optimization, this raises the question of correct beam dynamics simulations in presence of the nonlinearities that affect particle motion : fringe fields, multipolar defects in the lattice combined function (dipole + quadrupole) magnets, large amplitude motion.

For these reasons, we resort to stepwise ray-tracing. The goals of the present work are, to show the outcomes one can expect from ray-tracing means, to give preliminary results concerning large bunch dynamics in EMMA, and to establish basis data and procedures for possible further studies concerning field and alignment defects. In that, the present study is not very different from earlier ones based on matrix or other drift-kick methods [1, 2], with the advantage that it is based on realistic magnetic field models, as well as on accurate large amplitude tracking, yielding reliable knowledge of dynamic apertures.

FIELDS AND CELL PARAMETERS

EMMA lattice is based on a unique type of cell, a quadrupole doublet with two straight sections, one short and one long for, in particular, allowing space for RF cavities (Fig. 1). This lattice has been subject to extensive studies and publications [1, 3]. The set of parameters considered are summarized in Tab. 1.

The focusing (F) and defocusing (D) quadrupoles in the doublet cell are positioned radially so to ensure the bending - and orbit closure - at all energy, they act as combined function dipoles, with alternating bend sign over most of the energy span. The longitudinal phase slip is minimized, a key criterion for efficient use of fixed frequency RF. This correlates to optimization of the dispersion function, with

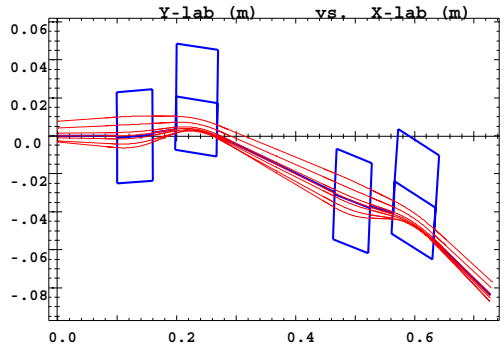

Figure 1: Closed orbits from 10 to 20 MeV (inner to outer trajectories) in a pair of FD cells. RF cavities are located in the long straight.

Table 1: Cell parameters. Bends are treated as straight multipoles with dipole component and gradient, radially displaced.

Optical element	Length (m)	Dipole component (T)	Gradient (T/m)
BF	0.06	-0.050721	7.4286
BD	0.07	0.074852	-4.6195
short drift	0.04		
long drift	0.2		

the beneficial effect of reduced overall transverse excursion during acceleration (which determines the horizontal optical aperture). Fig. 2 shows the corresponding evolution of magnetic field shape across the cell depending on energy. Closed orbit dependence on energy, a specific property of FFAGs, shows a general behavior of outward spiraling from injection to top energy (Fig. 1).

The focusing strength decreases with energy (natural chromaticity - sextupoles are avoided so to preserve large dynamic aperture), with behavior as shown in Fig. 3. the largest cell tunes, corresponding to lowest energy, are taken below the half integer, whereas the high energy tunes are kept reasonably high.

The cell geometry also ensures, in the present optics, the working hypothesis of identical time of flight (TOF) at both injection and extraction energies ; on the other hand it results from the longitudinal dynamic that the overall TOF behavior is almost quadratic in momentum difference $\delta \equiv \delta p/p$ (and but weak higher order dependence in δ), see Fig. 3, which also compares the linear parameters in presence of, or without fringe fields. The change in vertical tune due to non-zero fringe field extent, is weak, and however can be recovered from matrix methods by us-

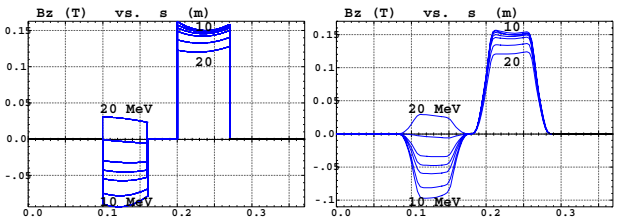

Figure 2: Field on closed orbits along the cell, at various energies, in the sharp-edge (left) or fringe field (right) magnet model.

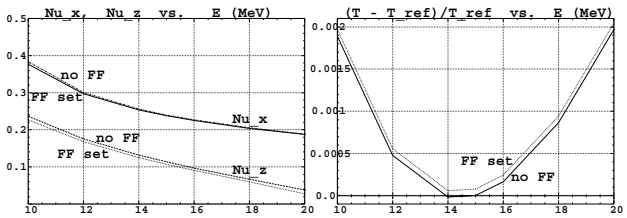

Figure 3: Left : Cell tunes as a function of energy. Right : $(T - T_{Ref})/T_{Ref}$ as a function of energy.

ing appropriate extent parameter (f) in the focusing term $(z'/z) = -\tan(w)/\rho + f/(6\rho^2\cos(w))$ (w = wedge angle, ρ = curvature radius).

STABILITY LIMITS

Fig. 4 shows the limit horizontal phase space trajectories at various energies, in case of pure horizontal motion, or including quasi-zero z motion, with or without fringe fields. The presence of arbitrarily small z motion substantially decreases the DA. The presence of fringe fields with 4-D motion tends to increase the DA, in case of coupled motion ; examination of tunes vs. amplitude shows that this effect could be correlated to a different behavior of the amplitude detuning.

The fact that the invariants shown in Fig. 4 are very thin gives confidence in the symplectic behavior of the integration. In particular, an increase of initial particle position by about a % in the vicinity of the invariants shown, results in the particle being kicked off (lost), without showing any fuzzy behavior.

LONGITUDINAL MOTION

Serpentine

Fig. 5-(top, left) shows acceleration of an initially elliptical ring, for zero transverse emittance. The ellipse contour is positioned in phase at start (close to π) so as to accelerate from 10 to 20 MeV. Fig. 5-(top, left) shows the final shape of the bunch contour, depending on the initial value of the ellipse orientation parameter, α, a possible variable in attempts to optimize the transmission.

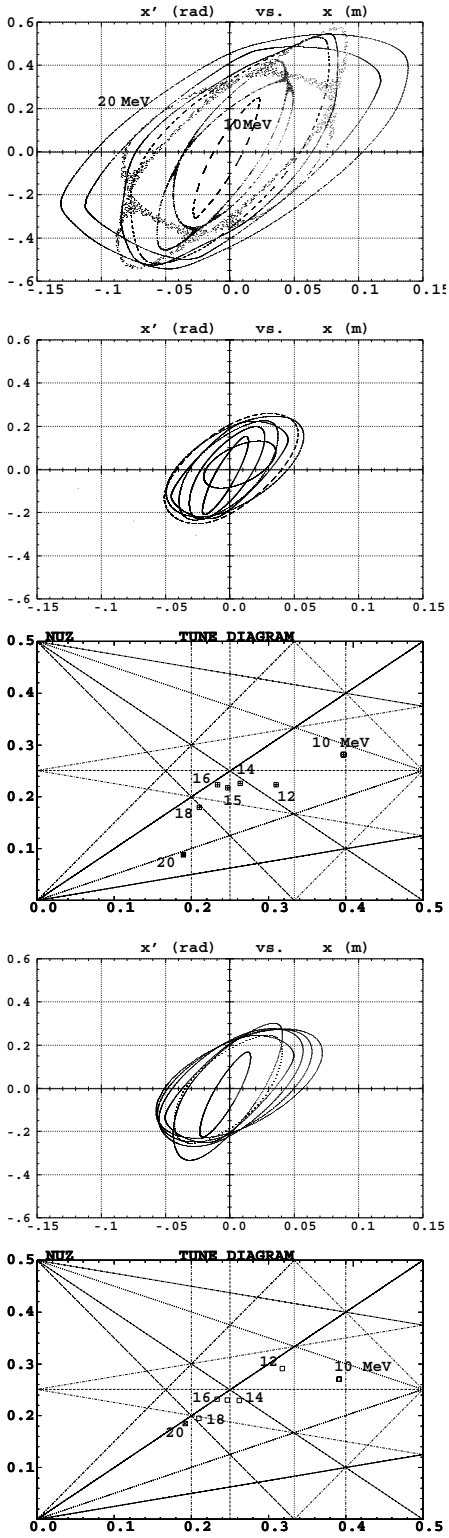

Figure 4: 2-D motion (x, x'), stability limits for 2000 cell passes, with about 5% precision in x, at 10, 12, 14, 15, 16, 18 and 20 MeV (from inner to outer invariant on left graph), and corresponding cell tunes at stability limits (resonance lines up to 5th order are represented). From top to bottom : (i) pure horizontal motion, no fringe fields, (ii) in presence of very small z motion, no fringe fields, (iii) corresponding tunes, (iv) in presence of very small z motion, fringe fields set, (v) corresponding tunes.

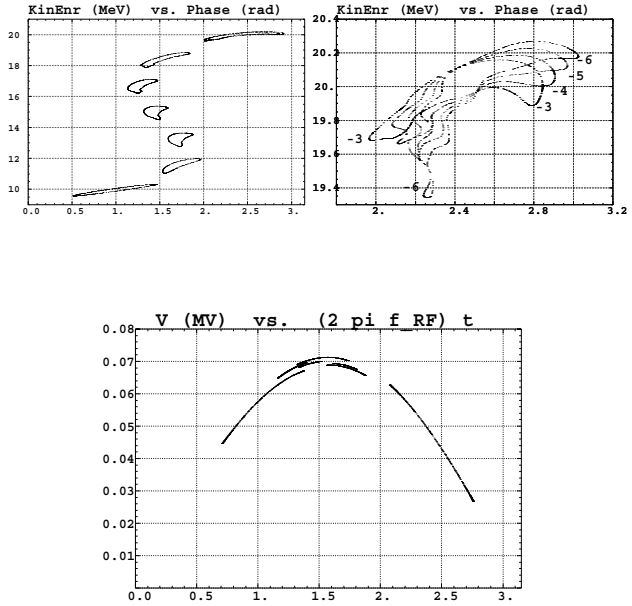

Figure 5: Acceleration of elliptical rings (zero transverse emittances) from 10 to 20 MeV in 125 cavity passes. Ellipses are represented each 25 cavity passage. Three particular trajectories show the separatrix and the bunch cog. Voltage : 70 kV peak, RF freq. : 1.3552 GHz. The right plot shows possibilities of optimization of the final longitudinal bunch shape, for instance here by varying the initial ellipse tilt, $-6 \leq \alpha_l \leq -3$. Bottom plot : projection of the bunch on the RF wave, at 4 distinct instants - the crest is crossed 3 times.

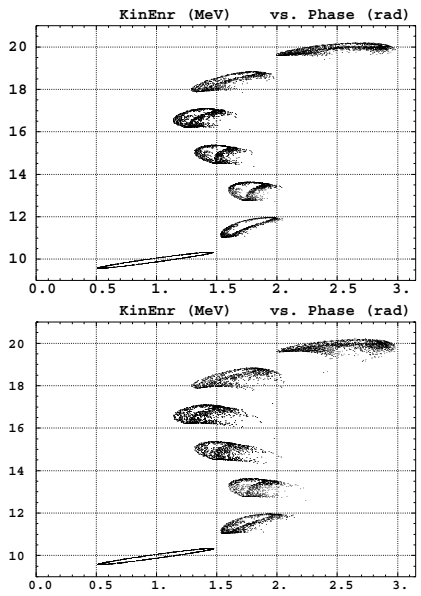

Figure 6: The sensible effect of launching a bunch with non-zero transverse size. Left : $\beta\gamma\epsilon_x/\pi \approx 1.4$ mm, right : $\beta\gamma\epsilon_x/\pi \approx 2.8$ mm. $\epsilon_z = 0$ in both cases.

6-D transmission

The working hypothesis for this 6-D tracking are : one cavity every 3 other cell, 80 kV per cavity, $f_{RF} = 1.356$ GHz. The top energy is attained in about 220 pass in the cavities.

5000 particles are tracked, initial 6-D phase space conditions are : about parabolic distribution in $\epsilon_{x,z} \approx 70\,10^{-6}\pi$ m.rad, and $\epsilon_l \approx 0.25\,10^{-4}\pi$eV.s ($\pm 0.125$ ns, ± 0.2 MeV).

Transverse behavior is shown in Fig. 7. Longitudinal behavior is similar to Fig. 6-right.

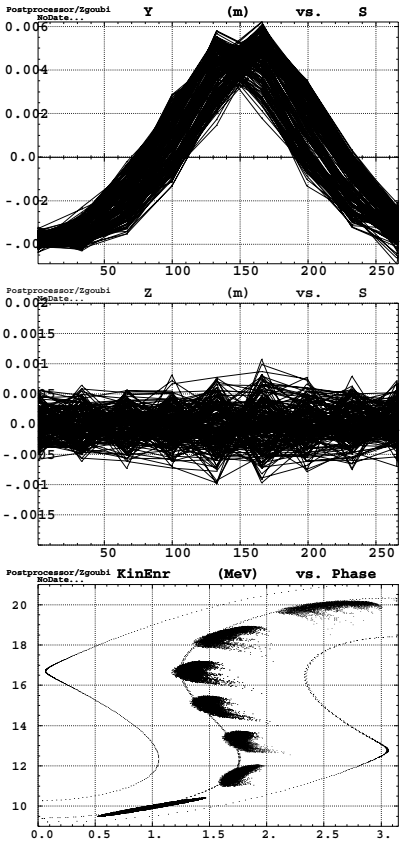

Figure 7: From top to bottom : (i) x-s and (ii) z-s during acceleration/deceleration (i.e., a full longitudinal period), observed along the ring at the location of the 14 cavities, (iii) longitudinal motion ; the plot also shows 2 trajectories close to the separatrix, and a third, central one.

REFERENCES

[1] http://hepunx.rl.ac.uk/uknf/wp1/emodel/.

[2] http://www.cap.bnl.gov/mumu/project/ISS/.

[3] http://slap.web.cern.ch/slap/NuFact/NuFact/NFNotes.html.

[4] E-model with RF systems at 1.3 GHz, E. Keil, CERN NuFcat Note 146 (2005).

[5] O CAMELOT ! A Memoir Of The MURA Years (Section 7.1), F.T.Cole, Proc. Cycl. Conf, April 11, 1994 ; FFAG particle accelerators, K.R. Symon et als., Phys.Rev. Vol.103-6, 1837-1859, 1956.

[6] Zgoubi users' guide, F. Méot and S. Valero, FERMILAB-TM-2010 (1997). See also, NIM A 427 (1999) 353-356.